Orientational order/disorder and network flexibility in deuterated methylammonium lead iodide by neutron total scattering: Supplementary Information

Jiaxun Liu,[1] Juan Du,[1] Anthony E Phillips,[1,*] Peter B Wyatt,[2] David A Keen,[3] and Martin T Dove[4,5,6,1,†]

[1]*Centre for Condensed Matter and Materials Physics, School of Physics and Astronomy, Queen Mary University of London, Mile End Road, London, E1 4NS, UK*
[2]*School of Biological and Chemical Sciences, Queen Mary University of London, Mile End Road, London, E1 4NS, UK*
[3]*ISIS Facility, Rutherford Appleton Laboratory, Harwell Campus, Didcot, Oxfordshire, OX11 0QX, UK*
[4]*School of Computer Sciences, Sichuan University, No 24 South Section 1, Yihuan Road, Chengdu, People's Republic of China 610065*
[5]*School of Physical Sciences, Sichuan University, No 24 South Section 1, Yihuan Road, Chengdu, People's Republic of China 610065*
[6]*Department of Physics, School of Sciences, Wuhan University of Technology, 205 Luoshi Road, Hongshan district, Wuhan, Hubei, 430070, People's Republic of China*

S1. NEUTRON SCATTERING EXPERIMENTS

A. Experimental methods and data corrections

1. Experiments

All measurements were performed on the POLARIS diffractometer [1] at the ISIS pulsed spallation neutron source in the United Kingdom. The polycrystalline sample was contained within a thin-walled cylindrical can of diameter 8 mm. The sample temperature was controlled using cryostat below 300 K and furnace above 300 K. Long measurements for analysis of the total scattering spectrum were performed at temperatures of 10, 100, 155, 170, 293, 300, 320, 335, 350, 375, and 400 K. Shorter runs for analysis of the powder diffraction pattern were obtained at intermediate temperatures. For correction of the total scattering data, additional measurements were performed of the empty instrument, empty sample environment, and empty can within the sample environment, together with a calibration measurement from a vanadium rod.

2. Corrections of diffraction data

Diffraction data for crystallographic analysis were transformed using the MANTID software [2].

3. Corrections of total scattering data

The total scattering data were corrected and transformed for analysis using the GUDRUN package [3]. This accounts for sources of data attenuation and extraneous sources of neutron scattering and attempts to put the data onto an absolute scale. Some attempts are made to account for effects associated with inelastic scattering. These are particularly severe for scattering from light elements, and of course, half of the atoms in methylammonium lead iodide are deuterium (with a small fraction of the light hydrogen isotope). The result was that there was a clear inconsistency between the higher-Q data from different banks of detectors. Experience has shown that the effects of this have the largest impact on the lowest-r peaks in the pair distribution function.

B. Equations of total scattering

In this section we reproduce the main equations underpinning the interpretation of neutron total scattering data in our paper. We follow the formalism of two recent reviews [4, 5]. Some issues regarding nomenclature have been discussed explicitly in an earlier paper [6].

The standard Debye equation [7] for the intensity of scattering of radiation from a collection of atoms, taken as an average over all relative orientations of the sample with respect to the neutron beam, is given as

$$S(Q) = \frac{1}{N}\sum_j b_j^2 + \frac{1}{N}\sum_{j\neq k} b_j b_k \frac{\sin(Qr_{jk})}{Qr_{jk}} \qquad \text{(S1)}$$

where Q is the modulus of the scattering vector. For elastic scattering processes, $Q = 4\pi\sin\theta/\lambda$, where θ is half the scattering angle and λ is the neutron wavelength. b_j is the scattering factor for atom labelled j, and r_{jk} is the distance between atoms labelled j and k. N is the total number of atoms in the sample. In equation S1 we separate out the terms $j = k$ because they simply form a constant value. As noted elsewhere [5], some workers define $S(Q)$ with a different normalisation [6].

The summation over all pairs of atoms is better replaced by a sum over pairs of atom types. Accordingly we define the partial pair distribution function (partial PDF) by writing the number of atoms of type n lying within a spherical shell of thickness dr at a distance r

* a.e.phillips@qmul.ac.uk
† martin.dove@qmul.ac.uk

from an atom of type m as $4\pi r^2 \mathrm{d}r \times c_n\rho \times g_{mn}(r)$. It is easy to show that if the atomic distributions are completely random, it will follow that $g_{mn}(r) = 1$ since the number of atoms in the shell is merely density multiplied by the volume of the shell. The pair sum in equation S1 can be replaced by

$$\frac{1}{N}\sum_{j\neq k} b_j b_k \frac{\sin(Qr_{jk})}{Qr_{jk}} = 4\pi\rho \int \sum_{m,n} c_m c_n b_m b_n r^2 g_{mn}(r) \frac{\sin(Qr)}{Qr}\,\mathrm{d}r \tag{S2}$$

In the limit that $r \to \infty$, $g_{mn}(r) \to 1$, reflecting the fact that a shell of large radius will contain a more uniform sample of atoms. The Fourier transform of this constant-value high-r limit will give a delta function at $Q = 0$, and thus we write

$$i(Q) \;=\; 4\pi\rho \int \sum_{m,n} c_m c_n b_m b_n r^2 \left(g_{mn}(r) - 1\right) \frac{\sin(Qr)}{Qr}\,\mathrm{d}r \;=\; S(Q) - \sum_m c_m b_m^2 - S_0 \tag{S3}$$

where the second term on the right hand side is the term for $j = k$ in equation S1, and S_0 is the delta function at $Q = 0$ arising from the limiting value of $g_{mn}(r \to \infty)$. We now define the overall PDF as

$$D(r) = 4\pi\rho r \sum_{m,n} c_m c_n b_m b_n \left(g_{mn}(r) - 1\right) \tag{S4}$$

Thus we can rearrange equation S3 as

$$Qi(Q) = \int_0^\infty D(r)\sin(Qr)\,\mathrm{d}r \tag{S5}$$

This has the reverse transformation:

$$D(r) = \frac{2}{\pi}\int_0^\infty Qi(Q)\sin(Qr)\,\mathrm{d}r \tag{S6}$$

The formalism used here is discussed in more detail and compared with other formulations in reference 6.

S2. REVERSE MONTE CARLO SIMULATION

A. Basics of the Reverse Monte Carlo method

The Reverse Monte Carlo (RMC) method was performed using the program RMCprofile [9], version 6.7. Briefly, the RMC method adjusts the positions of the atoms in a periodically repeating box of fixed size using a standard Metropolis Monte Carlo algorithm, driven by the requirement to give the best agreement between a set of calculated and experimentally-measured functions. We define an agreement function as

$$\chi^2 = \sum_m \sum_j (y_{j,m}^{\mathrm{exp}} - y_{j,m}^{\mathrm{calc}})^2 / \sigma_m^2 \tag{S7}$$

where $y_{j,m}$ is the point labelled j in the data set m, and the superscripts indicate experimental or calculated values respectively. σ_m is a weighting for each data set. In principle, it should correspond to a point-by-point standard deviation on the data, but these may not be known following the data corrections and Fourier transform. The data sets we used are the scattering function $i(Q)$, the PDF $D(r)$ and one of the data sets used in the Rietveld refinement.

Within the RMC method, at each step an atom chosen at random is moved by a random amount up to some pre-defined maximum value. As a result, χ^2 will change by an amount of $\Delta\chi^2$. If $\Delta\chi^2 < 0$ the move is accepted. Otherwise, the move is accepted with probability $\exp(-\Delta\chi^2/2)$. Typically the RMC simulations are run for much longer than it takes for the value of χ^2 to settle to a minimum constant average value. In our RMC simulations, the RMC had around 340 accepted moves per atom, with a maximum allowed displacement of 0.05 Å applied to each atom. Thirty independent RMC simulations were performed for each data set.

Two types of restraints were used in the RMC simulations. The first, known as the 'distance windows', set maximum and minimum distance between specified pairs of neighbouring atoms. For nearest-neighbour Pb–I pairs the limits were 3.30–5.65 Å, and for nearest-neighbour I–I pairs the limits were 2.55–4.94 Å. A distance window with limits 1.38–1.65 Å was also applied to the C–N bond. The second restraint was the use of interatomic potential functions. These were applied to the C–N, C–H and N–H bonds using a Morse potential, and bond-angle terms for H–C–H, H–N–H, C–N–H and N–C–H. The total energy from these potentials was added to χ^2 in the RMC algorithm.

B. Setting up the initial configurations

The starting configurations were generated using the code RMCcreate (also know as data2config) [10]. The input for this is a trial crystal structure, usually extracted from Rietveld refinement, of the correct unit cell parameters for the given temperature. The method then generates a starting configuration as a supercell of the starting configuration. Typically we chose supercells with edge lengths as close to 50 Å as possible, achieving this for supercell sizes of $6 \times 4 \times 6$ for the orthorhombic phase, $6 \times 6 \times 4$ for the tetragonal phase, and $8 \times 8 \times 8$ for the cubic phase.

Only the orthorhombic phase has ordered atom positions, so for the other two phases we created an ordered orientation of the MA molecular ions, and a utility within RMCcreate was used to give random orientations to each of these molecular ions.

C. Examples of the RMC results

Representative datasets to illustrate the quality of the RMC agreements are shown in Figure S1. We show, for each phase, a comparison of the RMC calculation with each of the three data sets used.

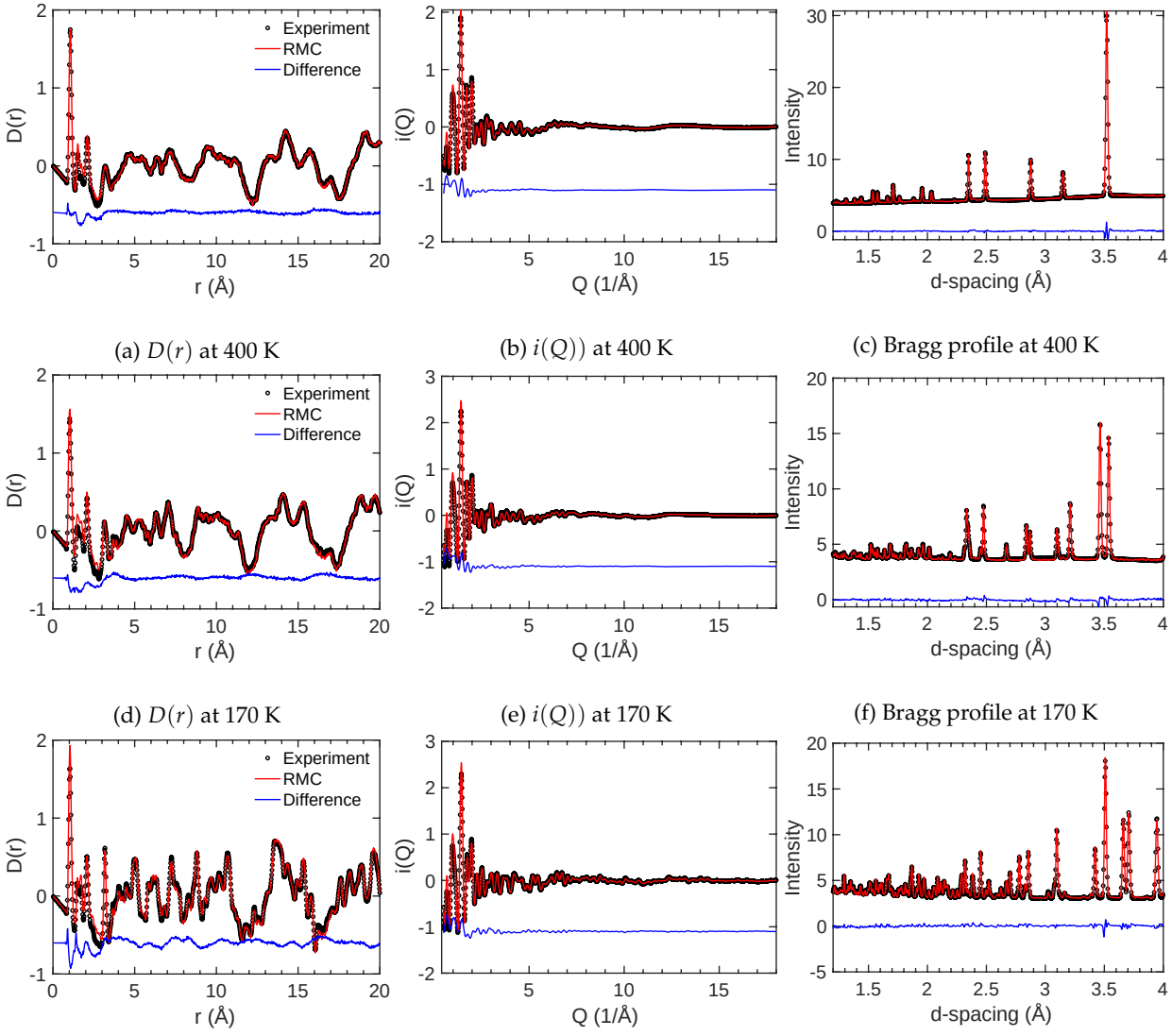

(a) $D(r)$ at 400 K (b) $i(Q))$ at 400 K (c) Bragg profile at 400 K

(d) $D(r)$ at 170 K (e) $i(Q))$ at 170 K (f) Bragg profile at 170 K

(g) $D(r)$ at 10 K (h) $i(Q))$ at 10 K (i) Bragg profile at 10 K

FIG. S1: The RMC fits to the experimental data used, including $D(r)$, $i(Q)$ and $I(t)$ for the high-temperature, room-temperature and low-temperature phases. The Bragg-scattering data have been transformed to d-spacing from time-of-flight.

S3. BOND ORIENTATIONAL DISTRIBUTION FUNCTION

A. Cubic symmetry

The orientational order/disorder of the MA cations can be described quantitatively by the bond distribution function $P(\Omega)$, where Ω is defined as the pair of polar angles (θ, ϕ) with θ as the zenith angle and ϕ as the azimuthal angle ($0 \leq \theta \leq \pi, 0 \leq \phi \leq 2\pi$). $P(\Omega)$ describes the probability of a C–N bond lying within a given element of solid angle $\mathrm{d}\Omega = \sin\theta\,\mathrm{d}\theta\,\mathrm{d}\phi$, normalised such that

$$\iint P(\Omega)\sin\theta\,\mathrm{d}\theta\,\mathrm{d}\phi = 1/4\pi \tag{S8}$$

For molecules lying on sites of cubic symmetry $m\bar{3}m$, it is convenient to expand $P(\Omega)$ in terms of the Kubic harmonic functions [11, 12]:

$$P(\Omega) = \frac{1}{4\pi}\sum_{\ell=0}^{\infty} c_\ell K_\ell(\Omega) \tag{S9}$$

where

$$K_0 = 1 \tag{S10a}$$

$$K_4 = \frac{\sqrt{21}}{4}(5Q - 3) \tag{S10b}$$

$$K_6 = \frac{\sqrt{13}}{8\sqrt{2}}(462S + 21Q - 17) \tag{S10c}$$

$$K_8 = \frac{\sqrt{561}}{32}\,(65Q^2 - 208S - 94Q + 33) \tag{S10d}$$

$$K_{10} = \frac{\sqrt{455}}{64\sqrt{2}}\,(7106QS + 187Q^2 - 3190S - 264Q + 85) \tag{S10e}$$

Here $Q = x^4 + y^4 + z^4$ and $S = x^2y^2z^2$, where $x = \sin\theta\cos\phi$, $y = \sin\theta\sin\phi$ and $z = \cos\theta$. For symmetry reasons terms with odd values of ℓ are absent, as also is the term for $\ell = 2$.

Because the functions K_ℓ are orthonormal, it follows that in the analysis of atomic configurations we can obtain the coefficients in equation S9 directly as $c_\ell = \langle K_\ell \rangle$, where the average is taken over all bonds in the RMC configuration, and over several independent configurations.

TABLE S1: c parameters for the high-temperature cubic phase.

ℓ	335 K	350 K	375 K	400 K
0	0.28209	0.28209	0.28209	0.28209
4	-0.00903	-0.02291	-0.01607	-0.02791
6	0.00197	-0.01405	-0.02612	-0.01320
8	-0.00384	-0.01247	-0.02809	0.00710
10	0.00205	0.01152	0.02389	0.00355

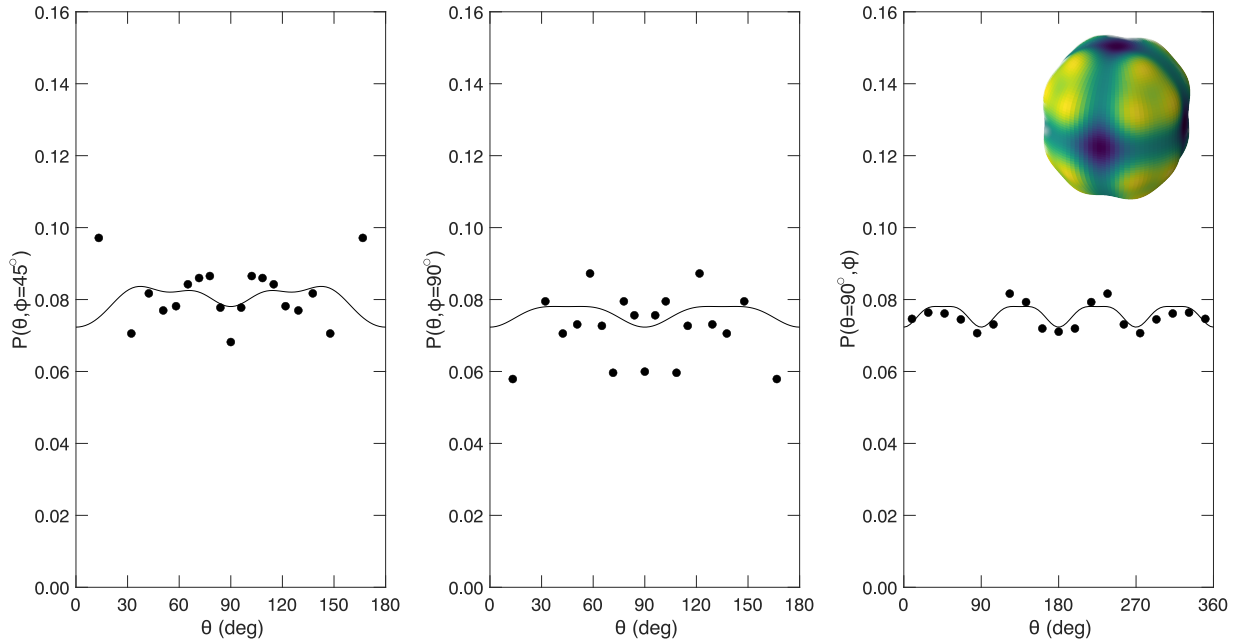

FIG. S2: The orientation distribution function $P(\Omega)$ of C–N bonds in the cubic phase of $MAPbI_3$ at 335 K obtained directly from the atomic configurations (black circles), with the corresponding function calculated using the derived Kubic harmonics (black lines) as described in the text. The value for completely random orientation distribution is $1/4 \simeq 0.08$. The inset shows the three-dimensional representation of the C–N orientational distribution function calculated from the Kubic harmonic functions.

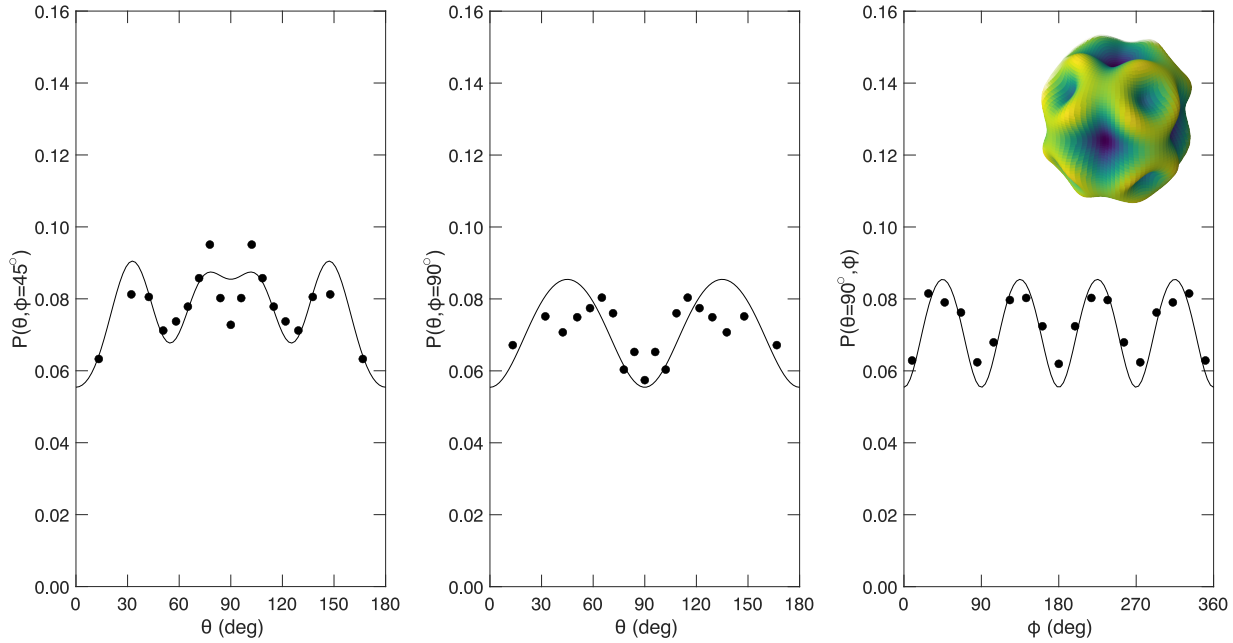

FIG. S3: The orientation distribution function $P(\Omega)$ of C–N bonds in the cubic phase of $MAPbI_3$ at 350 K obtained directly from the atomic configurations (black circles), with the corresponding function calculated using the derived Kubic harmonics (black lines) as described in the text. The value for completely random orientation distribution is $1/4 \simeq 0.08$. The inset shows the three-dimensional representation of the C–N orientational distribution function calculated from the Kubic harmonic functions.

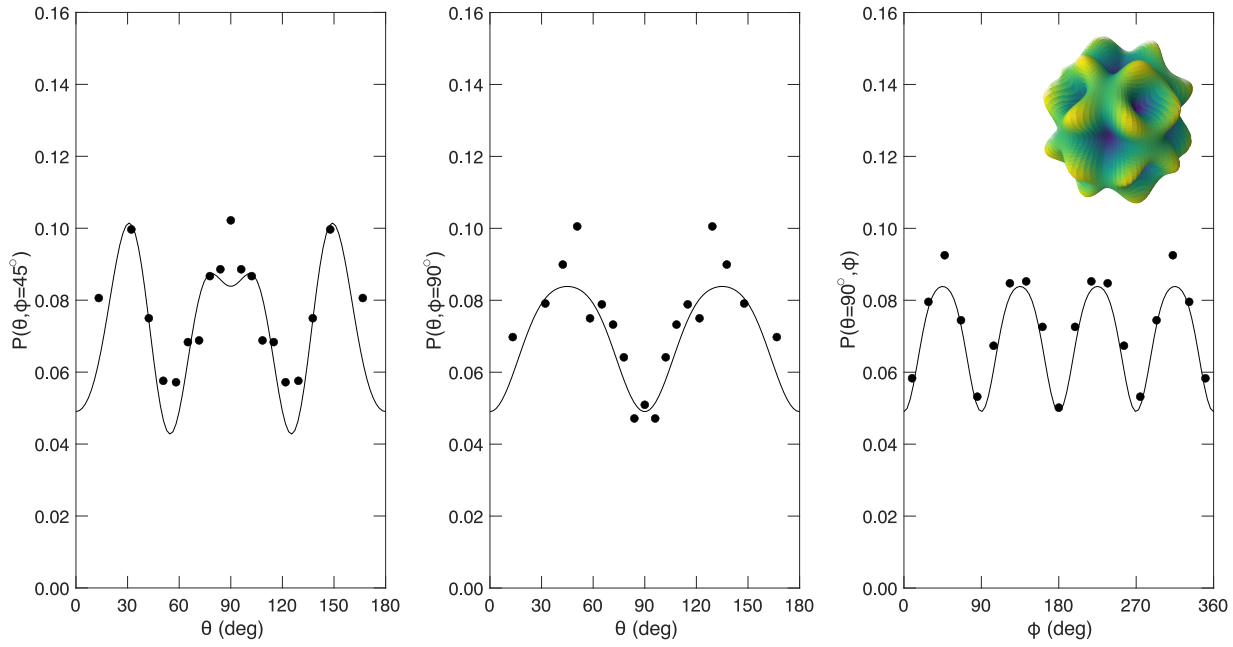

FIG. S4: The orientation distribution function $P(\Omega)$ of C–N bonds in the cubic phase of $MAPbI_3$ at 375 K obtained directly from the atomic configurations (black circles), with the corresponding function calculated using the derived Kubic harmonics (black lines) as described in the text. The value for completely random orientation distribution is $1/4 \simeq 0.08$. The inset shows the three-dimensional representation of the C–N orientational distribution function calculated from the Kubic harmonic functions.

TABLE S2: c parameters for the intermediate-temperature tetragonal phase.

ℓ	m	comb	170 K	293 K	300 K
0	0	c	0.28209	0.28209	0.28209
2	0	c	-0.08470	-0.03107	-0.03537
3	2	s	0.01523	-0.00105	0.00528
4	0	c	-0.03402	-0.00393	-0.00363
4	4	c	-0.07809	-0.03239	-0.02306
5	2	s	-0.00548	0.00156	0.00210
6	0	c	0.05217	0.02584	0.03198
6	4	c	-0.09502	-0.03996	-0.03275
7	2	s	-0.00814	0.00797	-0.00059
7	6	s	0.00085	-0.02033	0.00834
8	0	c	-0.02051	-0.01874	-0.01585
8	4	c	0.03293	-0.00742	0.00206
8	8	c	0.00757	-0.01216	-0.00623
9	2	s	0.01377	0.00538	0.00453
9	6	s	0.00047	-0.00135	0.00217
10	0	c	-0.00046	0.01066	0.01834
10	4	c	0.00852	0.01391	-0.01594
10	8	c	0.04847		0.00634

B. General symmetry

The main text has described the method to fit the C–N bond orientational distribution function using combinations of spherical harmonics to create real functions. The fitted coefficients for the tetragonal phase are given in Table S2, and for the orthorhombic phase in Table S3.

TABLE S3: c parameters for the low-temperature orthorhombic phase.

ℓ	m	comb	10 K	100 K	155 K	ℓ	m	comb	10 K	100 K	155 K
0	0	c	0.28209	0.28209	0.28209	10	10	c	-0.25692	-0.11687	-0.06882
1	1	c	-0.00217	-0.01503	-0.01176	10	2	s	-0.00485	0.01918	0.02077
1	1	s	0.00164	-0.00440	-0.00362	10	4	s	-0.02828	0.00772	-0.01191
2	0	c	-0.30500	-0.29290	-0.28361	10	6	s	-0.05460	-0.04512	-0.07002
2	2	c	-0.25261	-0.25484	-0.24697	10	8	s	-0.04080	-0.07454	-0.06840
2	2	s	0.02407	0.03781	0.05388	10	10	s	0.04650	0.02157	0.07271
3	1	c	0.00174	0.01733	0.01090	11	1	c	-0.00328	0.02019	0.00246
3	1	s	-0.00153	0.00213	0.01314	11	1	s	-0.00275	-0.01399	0.02452
3	3	c	0.00125	0.01095	0.00713	11	3	c	-0.00684	0.03035	-0.00105
3	3	s	-0.00826	0.02671	0.01586	11	3	s	0.00061	-0.00295	0.00923
4	0	c	0.28404	0.24943	0.22384	11	5	c	-0.00384	-0.00410	-0.01766
4	2	c	0.20281	0.18867	0.17218	11	5	s	0.00419	0.01069	-0.00687
4	4	c	-0.29308	-0.23757	-0.22295	11	7	c	0.00274	-0.04080	-0.02985
4	2	s	-0.01666	-0.02843	-0.04155	11	7	s	0.00907	0.01997	-0.00346
4	4	s	0.03422	0.03147	0.07528	11	9	c	0.00600	-0.02703	-0.01324
5	1	c	-0.00102	-0.02038	-0.00932	11	9	s	0.01213	0.01448	-0.00418
5	1	s	0.00149	0.00072	-0.02428	11	11	c	-0.00458	0.04568	0.03521
5	3	c	0.00008	-0.01959	-0.00561	11	11	s	-0.00505	-0.00213	-0.00851
5	3	s	0.00481	-0.01570	-0.01102	12	0	c	0.14222	0.06051	0.03216
5	5	c	0.00658	0.05016	0.04337	12	2	c	0.09789	0.04489	0.01714
5	5	s	-0.00372	-0.02134	-0.01617	12	4	c	-0.11122	-0.03980	-0.02794
6	0	c	-0.25245	-0.19493	-0.15567	12	6	c	-0.21304	-0.08734	-0.03692
6	2	c	-0.17559	-0.14481	-0.11947	12	8	c	-0.08658	-0.03933	-0.01852
6	4	c	0.21093	0.14294	0.11457	12	10	c	0.15861	0.05912	0.01970
6	6	c	0.50489	0.39681	0.32549	12	12	c	0.29714	0.12620	0.02628
6	2	s	0.01015	0.02298	0.03401	12	2	s	0.01148	-0.01895	-0.01486
6	4	s	-0.02869	-0.01707	-0.04150	12	4	s	0.02825	-0.01764	0.00448
6	6	s	-0.11866	-0.15121	-0.22750	12	6	s	0.03781	0.02190	0.03919
7	1	c	-0.00020	0.02174	0.00639	12	8	s	0.01776	0.05420	0.03550
7	1	s	-0.00151	-0.00432	0.03082	12	10	s	-0.03863	0.00850	-0.02553
7	3	c	-0.00196	0.02638	0.00238	12	12	s	-0.10176	-0.10875	-0.11571
7	3	s	-0.00256	0.00774	0.00972	13	1	c	0.00412	-0.01794	-0.00233
7	5	c	-0.00491	-0.03053	-0.03142	13	1	s	0.00464	0.01724	-0.01797
7	5	s	0.00316	0.01543	0.00484	13	3	c	0.00839	-0.02813	-0.00081
7	7	c	-0.00523	-0.08293	-0.06441	13	3	s	-0.00172	0.00555	-0.00769
7	7	s	0.02929	0.00316	0.01176	13	5	c	0.00394	-0.00324	0.01053
8	0	c	0.21558	0.14194	0.09846	13	5	s	-0.00606	-0.00900	0.00775
8	2	c	0.14872	0.10508	0.07445	13	7	c	-0.00422	0.02315	0.01895
8	4	c	-0.17207	-0.09589	-0.06388	13	7	s	-0.00712	-0.02136	0.01164
8	6	c	-0.34327	-0.21958	-0.15939	13	9	c	-0.00600	0.02254	0.00747
8	8	c	-0.16209	-0.13809	-0.07838	13	9	s	-0.00618	-0.01866	0.00693
8	2	s	-0.00273	-0.01982	-0.02709	13	11	c	0.00299	-0.02342	-0.01873
8	4	s	0.02821	0.00481	0.02373	13	11	s	0.00363	-0.00267	0.02790
8	6	s	0.07624	0.08154	0.12034	13	13	c	0.02534	-0.06929	-0.03845
8	8	s	0.08504	0.13041	0.13453	13	13	s	0.03113	0.01355	0.02373
9	1	c	0.00178	-0.02144	-0.00363	14	0	c	-0.11128	-0.03375	-0.01404
9	1	s	0.00180	0.00900	-0.03017	14	2	c	-0.07688	-0.02521	-0.00312
9	3	c	0.00442	-0.02982	0.00073	14	4	c	0.08611	0.02177	0.02045
9	3	s	0.00077	-0.00132	-0.00962	14	6	c	0.16546	0.05057	0.01380
9	5	c	0.00421	0.01600	0.02476	14	8	c	0.06819	0.02063	-0.00440
9	5	s	-0.00333	-0.01235	0.00266	14	10	c	-0.11469	-0.04534	-0.00572
9	7	c	0.00036	0.06087	0.04424	14	12	c	-0.18613	-0.05805	-0.01600
9	7	s	-0.01473	-0.01382	-0.00845	14	14	c	-0.03869	-0.02067	0.00486
9	9	c	-0.00376	0.03640	0.01889	14	2	s	-0.01627	0.01662	0.00966
9	9	s	-0.02846	-0.00333	-0.00819	14	4	s	-0.02796	0.02234	-0.00073
10	0	c	-0.17771	-0.09657	-0.05845	14	6	s	-0.02520	-0.00745	-0.02061
10	2	c	-0.12227	-0.07144	-0.04027	14	8	s	-0.00211	-0.04255	-0.01747
10	4	c	0.13986	0.06365	0.03905	14	10	s	0.03493	-0.02386	0.01186
10	6	c	0.26974	0.13913	0.08170	14	12	s	0.05895	0.04047	0.04298
10	8	c	0.11020	0.07200	0.04956	14	14	s	0.02293	0.07567	0.02698

[1] S. Hull, R. Smith, W. David, A. Hannon, J. Mayers, and R. Cywinski, The Polaris powder diffractometer at ISIS, Physica B: Condensed Matter **180-181**, 1000 (1992).

[2] O. Arnold, J. C. Bilheux, J. M. Borreguero, A. Buts, S. I. Campbell, L. Chapon, M. Doucet, N. Draper, R. F. Leal, M. A. Gigg, V. E. Lynch, A. Markvardsen, D. J. Mikkelson, R. L. Mikkelson, R. Miller, K. Palmen, P. Parker, G. Passos, T. G. Perring, P. F. Peterson, S. Ren, M. A. Reuter, A. T. Savici, J. W. Taylor, R. J. Taylor, R. Tolchenov, W. Zhou, and J. Zikovsky, Mantid—Data analysis and visualization package for neutron scattering and μ SR experiments, Nuclear Inst. and Methods in Physics Research, A **764**, 156 (2014).

[3] A. K. Soper, *GudrunN and GudrunX : programs for correcting raw neutron and X-ray diffraction data to differential scattering cross section*, Tech. Rep. RAL-TR-2011-013 (Rutherford Appleton Laboratory, 2011).

[4] D. A. Keen, Total scattering and the pair distribution function in crystallography, Crystallography Reviews **26**, 141 (2020).

[5] M. T. Dove and G. Li, Review: Pair distribution functions from neutron total scattering for the study of local structure in disordered materials, Nuclear Analysis **1**, 100037 (2022).

[6] D. A. Keen, A comparison of various commonly used correlation functions for describing total scattering, Journal of Applied Crystallography **34**, 172 (2001).

[7] L. Gelisio and P. Scardi, 100 years of Debye's scattering equation, Acta Crystallographica Section A Foundations and Advances **72**, 608 (2016).

[8] As noted elsewhere [5], some workers define $S(Q)$ with a different normalisation [6].

[9] M. G. Tucker, D. A. Keen, M. T. Dove, A. L. Goodwin, and Q. Hui, RMCProfile: reverse Monte Carlo for polycrystalline materials, Journal of Physics: Condensed Matter **19**, 335218 (2007).

[10] M. T. Dove and G. Rigg, RMCgui: a new interface for the workflow associated with running Reverse Monte Carlo simulations, Journal of Physics: Condensed Matter **25**, 454222 (2013).

[11] G. Dolling, B. M. Powell, and V. F. Sears, Neutron diffraction study of the plastic phases of polycrystalline SF_6 and CBr_4, Molecular Physics **37**, 1859 (1979).

[12] W. R. Fehlner and S. H. Vosko, A product representation for cubic harmonics and special directions for the determination of the Fermi surface and related properties, Canadian Journal of Physics **54**, 2159 (1976).